

Reply to Editor Comments

(C and R denote comment and reply, respectively)

We would like to express our sincere gratitude to you for your careful reading of our manuscript and for providing insightful and constructive comments. We have carefully considered all the comments and revised the manuscript accordingly. Below, we provide a detailed response to each comment raised by the editor.

Editor:

General comments:

C1: The authors present the analysis of rainfall and seismic data and infrared images recorded during 3 debris-flow events in two different catchments in China, each recorded with 2 different seismic station and infrared camera. In particular, they use spectral analysis of seismic data to extrapolate information of the events and also apply cross-correlation analysis to estimate flow velocity. Despite the work offering good quality seismic data of debris flow activity, most of the analysis and conclusions do not seem convincing and the work lacks novelty compared to previous contributions. More specifically, even if and not an expert in modelling of seismic propagation, I am not convinced at all about the reconstruction of the original seismic signal removing the propagation effects; it is not clear if authors considered geometrical spreading, inelastic absorption and or site effects and their approach, limited to considering only a short channel section does not appear to be robust or acceptable. In addition, many conclusions derived from the spectral features of the recorded seismic signals sound highly speculative and poorly supported by experimental or theoretical evidence to me.

R1: Thank you very much for your valuable comments. Based on the reviewer's suggestions, we have revised the research content, shifting the focus from monitoring and early warning to debris flow process reconstruction and characteristic analysis. As a result, we successfully reconstructed the second debris flow event at Fotangba.

Since we did not perform a station-to-station comparison, the geometrical spreading only restores the amplitude, and the compensation value is the same for a single receiving station. If a multi-station comparison is required, we would need to perform such a comparison. However, in this study, we primarily analyzed the data from a single station at different times and did not apply compensation to it.

Regarding inelastic absorption, the absorption rate varies across different frequencies for the same station. Therefore, it is essential to recover as much of this effect as possible. While the PSD theoretical model accounts for absorption factors, the PSD calculation model does not. Hence, we need inelastic absorption compensation to bridge this gap and help us better analyze the changes in debris flow characteristic parameters. Although the Q-value is included in our compensation algorithm, the algorithm itself is stable and can achieve stability through gain control values.

C2: I am also not convinced about the stress given on the use of the proposed system for monitoring and early warning purposes. If on one hand the use of seismic signals already proved to be a promising and effective tool for monitoring and early warning of debris flows, on the other hand, the system here presented, also lacking real time transmission of recorded data does not demonstrate any use for real time monitoring, despite authors recall several time to the demonstrated use of their system for the real time monitoring. No real time detection system is presented. I would suggest therefore toning this down and simply say that the paper suggests once more that seismic sensors could be used for debris flow warning, in agreement with previous events.

R2: Thank you very much for your valuable comments. Based on the reviewer's suggestions, and due to the limitations of network conditions, the on-site monitoring equipment was unable to transmit data in real-time. As a result, we have adjusted the focus of this study. Instead of emphasizing monitoring and early warning, we now focus on analyzing the characteristics of debris flow seismic signals. By combining images and field investigations, we have successfully reconstructed the second debris flow event at Fotangba.

C3: Furthermore, the text is too long and difficult to follow, also presenting long trivial and repetitive sections, and despite it being long, lacks important information on instrumental set up, seismic source process, and data analysis. No information is for example given on sensor type (1d or 3d seismometers or geophones, brands, response ecc). Similarly, the method section results confused, offering superfluous mathematical details while lacking explanation of the analysis actually conducted in the framework of the paper (e.g. window of analysis in spectral and cross correlation analysis). I also found difficult to understand why (to get which information or to investigate what) are same analysis conducted in the study.

R3: Thank you very much for your valuable comments. Based on your suggestions, we have revised the entire paper, removing redundant and repetitive sections. Additionally, we have included relevant instrument parameters (Table 1) and provided an introduction to the seismic signals used in cross-correlation. The specific changes are as follows:

Table 1 Instrument parameters for observation stations in the two study catchments.

Equipment	Instrument parameters	
	Fotangba Gully	Er Gully
Seismograph	Sampling rate 100 Hz	—
	Corner frequency not offered	
	Channel: Three components	
	Sensor type: Capacitive force balance pendulum	

<hr/> Dynamic range: Greater than 140 dB Bandwidth: 10 s - 50 Hz Sensitivity: 2000 V/(m/s)		
Geophone	—	Sampling rate 100 Hz Corner frequency of 4.5–150 Hz Type: Delta-Sigma 24 Bit Channels: Three components Dynamic range: 125db @ 100sps (128db @ 50sps) Noise level: 10nV/sqrt (Hz) Input impedance: 100kOhm
Instrument response	Voltage sensitivity: 2000V·S/m Normalized coefficient: 98696 Zero point: $z1=0.0+0.0i$ $z2=0.0+0.0i$ Main Pole: $p1=-0.444221-0.6565i$ $p2=-0.444221+0.6565i$ $p3=-222.110595-222.17759i$ $p4=-222.110595+222.17759i$	Logger: "Cube3ext", Gain: 16 (DATA-CUBE³ User Manual)
Rain gauge	Record once per hour with a resolution of 0.2 mm	
Infrared camera	1 shot every 5 minutes at 2592×1944, 1920×1080 dpi resolution during the day and at night	

Lines 614 to 618

The sampling rate for seismic signal monitoring is 100 Hz. The average amplitude for each second of seismic data is calculated using the amplitude method ([Arattano, 1999](#)), whereby 100 seismic signals are recorded within each second and their amplitudes are averaged. This method helps to smooth out high-frequency noise and provides a more stable representation of the amplitude of the seismic signal.

C4: In addition, the introduction focuses on debris flow monitoring and goes on the difficulties of deployments in poorly accessible sites. I think that a section on seismic source processes, presenting the accepted models on debris flow seismicity, is missing in the introduction: authors use seismic signal to invert for debris flow dynamics and features, so this section should be present. Finally, many sentences need to be linguistically revised and reworded. All text also requires to be shortened.

R4: Thank you very much for your valuable comments. We have shifted the focus of the study from monitoring and early warning to debris flow process reconstruction. Therefore, the section discussing the difficulties related to instrument deployment has

been removed. Additionally, we have added relevant content on the debris flow source model to the “[Introduction](#)” section, as follows:

Lines 131 to 153

The generation of debris flow seismic signals is closely related to the forces acting on the riverbed by the debris flow. Existing physical models of debris flow seismic sources are mainly derived from the theory of river transport and the theory of particle impact on the bed, and are closely related to the base forces acting on the riverbed ([Tsai et al., 2012](#); [Burtin et al., 2014](#); [Farin et al., 2019](#); [Zhang et al., 2021](#)). However, since the particle impact on the riverbed during debris flow movement is extremely complex, there is currently no universally applicable debris flow seismic source model. [Lai et al. \(2018\)](#) suggested that high-frequency seismic signals from debris flows are closely related to the area of the head zone, the particle size contained in the debris flow, and the average flow velocity of the head zone. However, this model also assumes vertical particle impacts on the ground, neglecting the influence of channel shape and topographic variations on the particle impact angle. [Kean et al. \(2015\)](#) found that the sediment cover on the debris flow bed strongly suppresses ground vibrations. [Bell et al. \(2025\)](#) proposed that, in addition to particle collisions, turbulence also radiates seismic waves within the debris flow.

Although the debris flow seismic source model is not yet fully understood, experimental results from [Allstadt et al. \(2020\)](#) demonstrated that high-frequency seismic signals from debris flows can reflect overall movement characteristics, such as flow depth, gravity, density, momentum, and kinetic energy. The seismic signals generated during the debris flow process contain rich information about debris flow parameters (e.g., flow depth, particle size, flow velocity). Therefore, using seismic signals to reconstruct the debris flow process is a reliable method.

References

- Kean, J. W., Coe, J. A., Coviello, V., Smith, J. B., McCoy, S. W., Arattano, M., 2015. Estimating rates of debris flow entrainment from ground vibrations. *Geophysical Research Letters*, 42(15), 6365-6372.
- Zhang, Z., Walter, F., McArdell, B. W., Wenner, M., Chmiel, M., de Haas, T., He, S., 2021. Insights from the particle impact model into the high-frequency seismic signature of debris flows. *Geophysical Research Letters*, 48(1), e2020GL088994.

- Belli, G., Marchetti, E., Walter, F., Gheri, D., 2025. Infrasound unmasks flow turbulence as an additional seismic source in debris flows. *Geophysical Research Letters*, 52(8), e2025GL116107.
- Burtin, A., Hovius, N., McArdell, B. W., Turowski, J. M., Vergne, J., (2014). Seismic constraints on dynamic links between geomorphic processes and routing of sediment in a steep mountain catchment. *Earth Surface Dynamics*, 2(1), 21-33.
- Allstadt, K. E., Farin, M., Iverson, R. M., Obryk, M. K., Kean, J. W., Tsai, V. C., Logan, M., 2020. Measuring basal force fluctuations of debris flows using seismic recordings and empirical green's functions. *Journal of Geophysical Research: Earth Surface*, 125(9), e2020JF005590.
- Farin, M., Tsai, V. C., Lamb, M. P., Allstadt, K. E., 2019. A physical model of the high-frequency seismic signal generated by debris flows. *Earth Surface Processes and Landforms*, 44(13), 2529-2543.
- Tsai, V. C., Minchew, B., Lamb, M. P., & Ampuero, J.-P., 2012. A physical model for seismic noise generation from sediment transport in rivers. *Geophysical Research Letters*, 39(2), L02404.

Specific comments:

C1: Title: Real-time monitoring? You don't perform any real time monitoring, please remove this from the title.

R1: Thank you very much for your valuable comments. We have deleted the content about real-time monitoring.

C2: Introduction:

A section on the seismic source process in debris flow is missing (view Burtin 2009, 2014 Lai 2018, Kean 2015, Zhang 2021, Belli 2025...). Shorten the parts referring to hard access to DF sites.

R2: Thank you very much for your valuable comments. We have added content about the seismic source process, as follows:

Lines 131 to 153

The generation of debris flow seismic signals is closely related to the forces acting on the riverbed by the debris flow. Existing physical models of debris flow seismic sources are mainly derived from the theory of river transport and the theory of particle impact on the bed, and are closely related to the base forces acting on the riverbed (Tsai et al., 2012; Burtin et al., 2014; Farin et al., 2019; Zhang et al., 2021). However, since the particle impact on the riverbed during debris flow movement is extremely complex, there is currently no universally applicable debris flow seismic source model. Lai et al. (2018) suggested that high-frequency seismic signals from debris flows are closely

related to the area of the head zone, the particle size contained in the debris flow, and the average flow velocity of the head zone. However, this model also assumes vertical particle impacts on the ground, neglecting the influence of channel shape and topographic variations on the particle impact angle. [Kean et al. \(2015\)](#) found that the sediment cover on the debris flow bed strongly suppresses ground vibrations. [Bell et al. \(2025\)](#) proposed that, in addition to particle collisions, turbulence also radiates seismic waves within the debris flow.

Although the debris flow seismic source model is not yet fully understood, experimental results from [Allstadt et al. \(2020\)](#) demonstrated that high-frequency seismic signals from debris flows can reflect overall movement characteristics, such as flow depth, gravity, density, momentum, and kinetic energy. The seismic signals generated during the debris flow process contain rich information about debris flow parameters (e.g., flow depth, particle size, flow velocity). Therefore, using seismic signals to reconstruct the debris flow process is a reliable method.

References

- Kean, J. W., Coe, J. A., Coviello, V., Smith, J. B., McCoy, S. W., Arattano, M., 2015. Estimating rates of debris flow entrainment from ground vibrations. *Geophysical Research Letters*, 42(15), 6365-6372.
- Zhang, Z., Walter, F., McArdell, B. W., Wenner, M., Chmiel, M., de Haas, T., He, S., 2021. Insights from the particle impact model into the high-frequency seismic signature of debris flows. *Geophysical Research Letters*, 48(1), e2020GL088994.
- Belli, G., Marchetti, E., Walter, F., Gheri, D., 2025. Infrasound unmasks flow turbulence as an additional seismic source in debris flows. *Geophysical Research Letters*, 52(8), e2025GL116107.
- Burtin, A., Hovius, N., McArdell, B. W., Turowski, J. M., Vergne, J., (2014). Seismic constraints on dynamic links between geomorphic processes and routing of sediment in a steep mountain catchment. *Earth Surface Dynamics*, 2(1), 21-33.
- Allstadt, K. E., Farin, M., Iverson, R. M., Obryk, M. K., Kean, J. W., Tsai, V. C., Logan, M., 2020. Measuring basal force fluctuations of debris flows using seismic recordings and empirical green's functions. *Journal of Geophysical Research: Earth Surface*, 125(9), e2020JF005590.
- Farin, M., Tsai, V. C., Lamb, M. P., Allstadt, K. E., 2019. A physical model of the high-frequency seismic signal generated by debris flows. *Earth Surface Processes and Landforms*, 44(13), 2529-2543.
- Tsai, V. C., Minchew, B., Lamb, M. P., & Ampuero, J.-P., 2012. A physical model for seismic noise generation from sediment transport in rivers. *Geophysical Research Letters*, 39(2), L02404.

C3: Line 37-38: I don't understand this sentence "a strong correlation between... spectrum"

R3: Thank you very much for your valuable comments. Due to changes in the research content, we have deleted this sentence.

C4: Highlights: the 3 highlights are not completed sentences; rephrase them all.

R4: Thank you very much for your valuable comments. We have made modifications. As follows:

Lines 32 to 43

Highlights:

- By analyzing the characteristics of seismic signals, the study successfully reconstructed the entire process of the second debris flow event at Futangba Gully by utilizing features such as the time series, flow velocity, particle characteristics, and surge variations of the debris flow.
- The seismic signal characteristics of the debris flow showed rapid excitation and slow attenuation. Even after removing propagation effects, significant differences in amplitude and frequency were observed at different monitoring stations, indicating changes in the dynamic parameters of the debris flow.
- The time-frequency characteristics of seismic signals reflect the evolution process of debris flows, with a corresponding relationship between the power spectral density and debris flow characteristics.

C5: Line 90-93: remove all lines 90, 91 and 92 and 93, leaving just "to monitor landslides (Li 207; Fuchs 2018), rockfalls..."

R5: Thank you very much for your valuable comments. We have made modifications. As follows:

Lines 105 to 109

Environmental seismology have been applied to monitor various geological events, including landslides (Li et al., 2017; Fuchs et al., 2018), rockfalls (Deparis et al., 2008; Vilajosana et al., 2008), avalanches (Schneider et al., 2010; Van Herwijnen and Schweizer, 2011), as well as debris flow (Arattano, 1999; Burtin et al., 2009; Schimmel and Hübl, 2016; Walter et al., 2017; Lai et al., 2018).

C6: Line 104-105: also Belli et al 2022 found a linear relation between seismic signals and flow depth/ discharge. Also change "rate" with "magnitude"

R6: Thank you very much for your valuable comments. We have made modifications.

As follows:

Lines 112 to 113

Belli et al. (2022) found that physical parameters (front velocity, maximum flow depth and density) of debris flows correlate positively with seismic signal amplitudes.

C7: Line 105-108: add “investigation of the source process” in the list and refer to Zhang et al., 2021

(<https://agupubs.onlinelibrary.wiley.com/doi/full/10.1029/2021JB022755>) and Belli et al. 2025

(<https://agupubs.onlinelibrary.wiley.com/doi/10.1029/2025GL116107?af=R>).

R7: Thank you very much for your valuable comments. We have added relevant content, which can be found in **R2**.

C8: Line 111-113: remove this period

Line 113-117: I suggest to remove also this period

R8: Thank you very much for your valuable comments. We have removed this period.

C9: 122-129: shorten this section

R9: Thank you very much for your valuable comments. Due to changes in the research content, we have deleted this section.

C10: 132: put a “.” after “camera” and start a new period with “The system recorded 3 debris flows...”

R10: Thank you very much for your valuable comments. We have made modifications. As follows:

Lines 154 to 157

This study is based on the characteristics of debris flows in the Wenchuan region of China and uses a near-field debris flow observation system consisting of seismic instruments, rain gauges, and infrared cameras. We collected data on three debris flows that occurred in Wenchuan on August 19, 2022.

C11: 137: semi-quantitative analysis of what?

R11: Thank you very much for your valuable comments. We have deleted this sentence.

C12: Section 2:

153-155: not clear if these events are included in the 17 cited before

R12: Thank you very much for your valuable comments. The 17 events mentioned here refer to those that occurred before 2016 and do not include the three events.

C13: Figure 1: put the stations in the map; sea boundaries of China in the panel a are not evident

R13: Thank you very much for your valuable comments. We have made modifications. As follows:

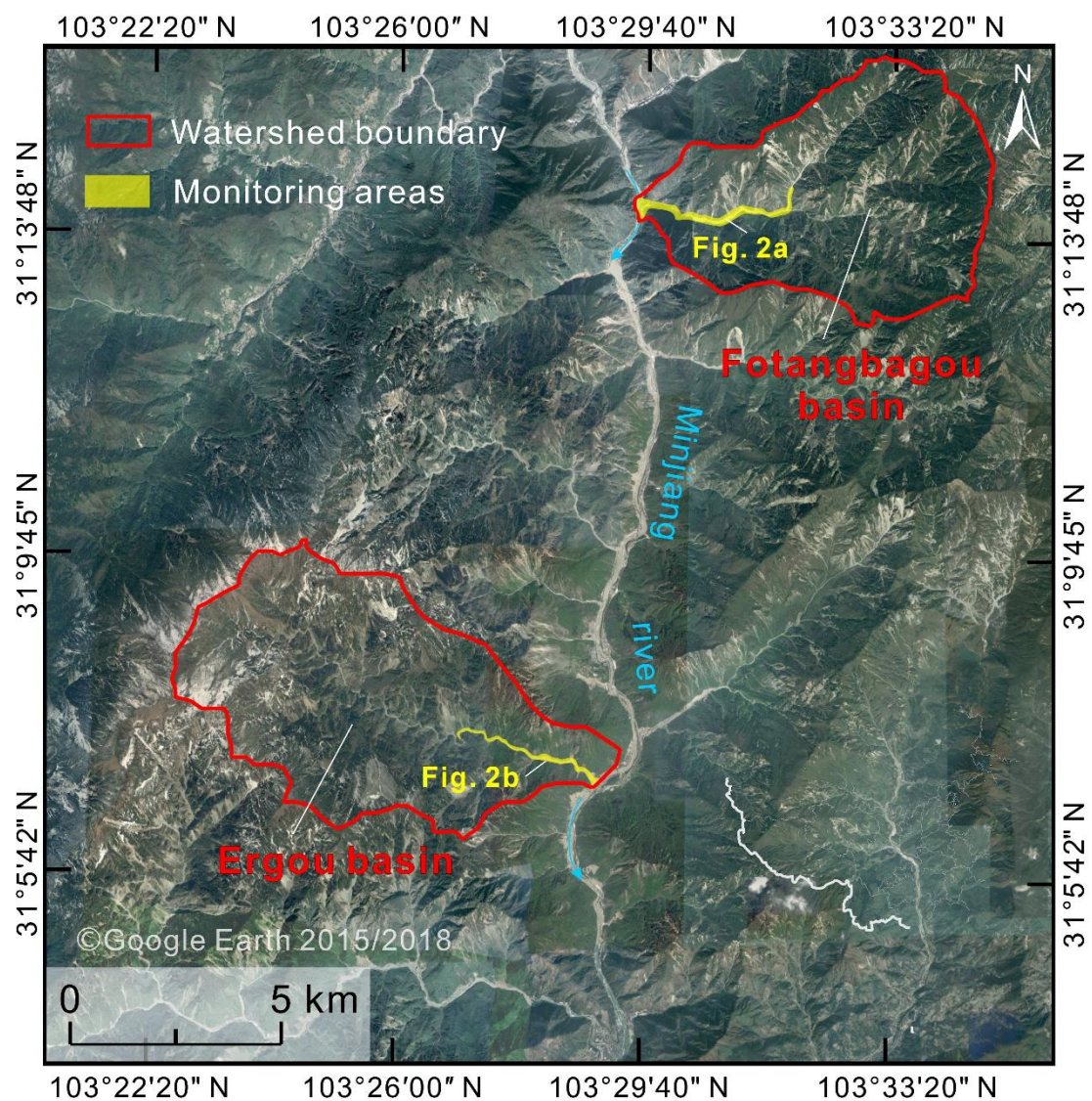


Fig. 1. The two study catchments, Er and Fotangba Gullies, on the Minjiang River, Wenchuan, Sichuan, China.

C14: 164-167: Slope is before 12° and then 15°.

R14: Thank you very much for your valuable comments. We apologize for the incorrect sentence. We have deleted it.

C15: 164-165: “a debris flow transportation area of between 5 and 12°”?

167-170: remove, already written at 150-152 and not relevant

175-176: remove, already written at 150-152 and not relevant

R15: Thank you very much for your valuable comments. We apologize for the error and repetition in the previous version. We have made the necessary revisions to clarify the content. The updated information is as follows:

Lines 185 to 190

Er Gully drains an area of 39.4 km² and is about 6 km from the epicenter of the Wenchuan Earthquake; it ranges in altitude from 930 to 4120 m, has a channel length of about 12 km, an average slope of about 12° (Guo et al., 2016). The Fotangba Gully basin has an area of 33.6 km²; it ranges in altitude from 1117 to 3462 m, has a channel length of about 9.78 km, with an average slope of 6.1°, and has bank slopes of 25° to 45° (Cao et al., 2019).

C16: Section 2.2: I suggest renaming this section “Instrumental set-up” or “observation system” or similar instead of “monitoring system”: a monitoring system requires real time alerting or warning and refers to surveillance purposes, and this is not the case. Change all the “monitoring system” referring to your instrumental set up in the text (e.g. line 207, 218, 220 ...).

R16: Thank you very much for your valuable comments. We have revised the content accordingly, changing the monitoring system to the observation system, and making additional modifications to the subsequent sections.

C17: Section 2.2: revise the all section: please provide sensors specifications (seismometer or geophone model, digitizer, camera ... Some of them are in the table which could be omitted then) and avoid trivial details on sensor deployment.

R17: Thank you very much for your valuable comments. Based on your suggestions, we have added the relevant instrument parameters in Table 1.

Table 1 Instrument parameters for observation stations in the two study catchments.

Equipment	Instrument parameters	
	Fotangba Gully	Er Gully
Seismograph	Sampling rate 100 Hz	
	Corner frequency not offered	
	Channel: Three components	
	Sensor type: Capacitive force balance	
	pendulum	—
	Dynamic range: Greater than 140 dB	
	Bandwidth: 10 s - 50 Hz	
Geophone	Sensitivity: 2000 V/(m/s)	
		Sampling rate 100 Hz
		Corner frequency of 4.5–150 Hz
		Type: Delta-Sigma 24 Bit
		Channels: Three components
		Dynamic range: 125db @ 100sps (128db @ 50sps)
		Noise level: 10nV/sqrt (Hz)
Instrument response		Input impedance: 100kOhm
	Voltage sensitivity:2000V·S/m	
	Normalized coefficient: 98696	
	Zero point: z1=0.0+0.0i	Logger: "Cube3ext",
	z2=0.0+0.0i	Gain: 16
	Main Pole: p1=-0.444221-0.6565i	(DATA-CUBE³ User Manual)
	p2=-0.444221+0.6565i	
Rain gauge	p3=-222.110595-222.17759i	
	p4=-222.110595+222.17759i	
	Record once per hour with a resolution of 0.2 mm	
Infrared camera	1 shot every 5 minutes at 2592×1944, 1920×1080 dpi resolution during the day and at night	

C18: 183-206: all this section is too long and results trivial and not so meaningful: I suggest reducing it in a very few lines stating how you faced the low insolation of the area with no further details (single costs ecc)

R18: Thank you very much for your valuable comments. Due to adjustments in the research content, this section has been removed.

C19: 210-211: and station 2?

R19: Thank you very much for your valuable comments. We have made modifications. As follows:

Lines 196 to 202

The Fotangba gully observation stations 1 and 2 are located 3,260 meters and 2,740 meters from the canyon entrance, respectively, while the Er gully Observation stations 1 and 2 are located 4,130 meters and 3,670 meters from the entrance (Table 1, Fig. 2). The distance between the two monitoring stations in Fotangba gully and Er gully is 520 meters and 460 meters, respectively. Both monitoring stations are installed on rocky platforms on the left bank of the river. The two observation stations in Fotangba gully are located approximately 20 meters and 15 meters from the centerline of the river.

C20: Section 3: Metodology: presenting the equations for FFT, PSD and cross-correlation functions appears superfluous to me, as these are well known techniques of analysis in geophysics. In addition the text is rather confused and difficult to follow. I would suggest removing the equations, rewriting the section in a simplified version more focused on your signal analysis and your scopes of investigations, rather than of mathematics and technical details. A structure like the following: “With the aim to investigate... we perform the XXXX analysis on seismic data... “

R20: Thank you very much for your valuable comments. We have modified the methodology section. As follows:

Lines 241 to 270

3.1 Power spectral density analysis

Tsai et al. (2012) developed a PSD model for sediment transport that links seismic signals with water turbulence, precipitation, and sediment transport in rivers. In their model, they considered the relationship between seismic signals and the transport of bedload in rivers. Tsai et al. (2012) adapted this model for debris flows by including absorption damping during the propagation process and established the PSD model for debris flows near the source shown in Eq. (1). This model links debris flow parameters such as length, particle size, width, velocity, and attenuation factors (due to absorption) as well as viscoelastic parameters during propagation with the seismic PSD of the debris flow.

$$PSD \approx 1.9 \cdot LWD^3 u^3 \cdot \frac{f^{3+5\xi}}{v_c^5 r_0} e^{-\frac{8.8 f^{1+\xi} \eta}{v_c Q}}, \quad (1)$$

where W is width of the channel, D represents the 94th centile of the grain size distribution, u represents debris flow velocity, f is frequency, v_c is Rayleigh wave phase velocity at 1 Hz, r_0 is distance between the monitoring station and channel, L is effective length of $L=r_0$, $\xi=0.4$ is a parameter related to how strongly seismic velocities increase with depth at the site, and Q is an attenuation factor (Tsai et al., 2012; Lai et al., 2018).

Debris flow seismic Power spectral density calculated by Eq. (2), which means the power per frequency for different frequencies in a specific period (Yan et al., 2020), and allows debris flow evolution to be analyzed from the seismic signal. The power of full band seismic is calculated by the short-time Fourier transform (STFT, Eq. 3), allowing getting the frequency domain characteristics of the signal versus time, which can help us to get the PSD changes versus the time.

$$PSD_{f_{\min} \sim f_{\max}}(t) = \frac{1}{(f_{\max} - f_{\min})} \times \sum_{f=f_{\min}}^{f_{\max}} X(t, f), \quad (2)$$

$$X(t, f) = \sum_{-\infty}^{\infty} x(m)W(t - m)e^{-j2\pi fm} \quad (3)$$

where f is the angular frequency, f_{\min} and f_{\max} represent minimum frequency and maximum frequency, respectively, t is time for the seismic signal, $X(t, f)$ represents the spectrogram based on STFT (Yan et al., 2017)., x are time domain signals, W is the window function, m is the start time of the window function, e is a natural constant, t is time, and j is the imaginary number (Yan et al., 2021). A Hanning window length of 2056 and a time length of 20.56 s correspondingly is used. A built-in function “spectrogram” of MATLAB is used to achieve STFT directly from the software manual. The sampling rate is 100 Hz, so we choose 1 Hz and 50 Hz (i.e., a half of 100 Hz) as f_{\min} and f_{\max} .

C21: 233-244: revise and rephrase all this section: the subject of the sentences is always missing

R21: Thank you very much for your valuable comments. We have made modifications. As follows:

Lines 215 to 222

With the aim to investigate to get the evolution of debris flow, we have designed the seismic signal processing and interpretation flow, as shown in Fig. 2. The power spectral density, time-frequency spectrum and simplified signal of the debris flow seismic signals by the compensated seismic data record by in-situ monitoring network in Fig. 2. The infrared imagery, Manning formula velocity, and other post-event on-site investigations will be used to validate the debris flow evolution reconstructed from the seismic signals. To achieve this, we designed a research methodology, as shown in Fig. 3.

C22: 240: what are “on site investigations?” specify

242: keyframes?

242: what is the amplitude method?

R22: Thank you very much for your valuable comments. We have made modifications, which can be found in **R21**.

C23: Figure 3: is this necessary?

R23: Thank you very much for your valuable comments. Fig. 3 is mainly the research flowchart, which clarifies the overall research process.

C24: Section 3.1: this section is unclear to me; I suggest to put 3.1 and 3.3 together in a single section and revise it just stating that seismic signals are analyzed in the frequency domain and spectra are computed in the form of PSD and spectrogram

253-258: remove the equation

R24: Thank you to the reviewer for the constructive suggestions. In this revision, we have rewritten the Methodology section. The first paragraph after the rewrite is as follows: " With the aim to investigate to get the evolution of debris flow, we have designed the seismic signal processing and interpretation flow, as shown in Fig. 2. The Power spectral density, time-frequency spectrum and simplified signal of the Debris flow seismic signals by the compensated seismic data record by in-situ monitoring network in Fig. 2. The infrared imagery, Manning formula velocity, and other post-event on-site investigations will be used to validate the debris flow evolution reconstructed from the seismic signals. To achieve this, we designed a research methodology, as shown in Fig. 3." We have combined the PSD theoretical model and the seismic data solution process, and due to the differences in absorption terms between the two, we introduce the need for absorption attenuation compensation. This

approach makes the Methodology section more logical. As follows:

Lines 215 to 222:

With the aim to investigate to get the evolution of debris flow, we have designed the seismic signal processing and interpretation flow, as shown in Fig. 2. The Power spectral density, time-frequency spectrum and simplified signal of the Debris flow seismic signals by the compensated seismic data record by in-situ monitoring network in Fig. 2. The infrared imagery, Manning formula velocity, and other post-event on-site investigations will be used to validate the debris flow evolution reconstructed from the seismic signals. To achieve this, we designed a research methodology, as shown in Fig. 3.

Lines 241 to 270

3.1 Power spectral density analysis

Tsai et al. (2012) developed a PSD model for sediment transport that links seismic signals with water turbulence, precipitation, and sediment transport in rivers. In their model, they considered the relationship between seismic signals and the transport of bedload in rivers. Tsai et al. (2012) adapted this model for debris flows by including absorption damping during the propagation process and established the PSD model for debris flows near the source shown in Eq. (1). This model links debris flow parameters such as length, particle size, width, velocity, and attenuation factors (due to absorption) as well as viscoelastic parameters during propagation with the seismic PSD of the debris flow.

$$PSD \approx 1.9 \cdot LWD^3 u^3 \cdot \frac{f^{3+5\xi}}{v_c^5 r_0} e^{-\frac{8.8 f^{1+\xi} \eta}{v_c Q}}, \quad (1)$$

where W is width of the channel, D represents the 94th centile of the grain size distribution, u represents debris flow velocity, f is frequency, v_c is Rayleigh wave phase velocity at 1 Hz, r_0 is distance between the monitoring station and channel, L is effective length of $L=r_0$, $\xi=0.4$ is a parameter related to how strongly seismic velocities increase with depth at the site, and Q is an attenuation factor (Tsai et al., 2012; Lai et al., 2018).

Debris flow seismic Power spectral density calculated by Eq. (2), which means the

power per frequency for different frequencies in a specific period (Yan et al., 2020), and allows debris flow evolution to be analyzed from the seismic signal. The power of full band seismic is calculated by the short-time Fourier transform (STFT, Eq. 3), allowing getting the frequency domain characteristics of the signal versus time, which can help us to get the PSD changes versus the time.

$$PSD_{f_{\min} \sim f_{\max}}(t) = \frac{1}{(f_{\max} - f_{\min})} \times \sum_{f=f_{\min}}^{f_{\max}} X(t, f), \quad (2)$$

$$X(t, f) = \sum_{m=-\infty}^{\infty} x(m)W(t - m)e^{-j2\pi fm} \quad (3)$$

where f is the angular frequency, f_{\min} and f_{\max} represent minimum frequency and maximum frequency, respectively, t is time for the seismic signal, $X(t, f)$ represents the spectrogram based on STFT (Yan et al., 2017)., x are time domain signals, W is the window function, m is the start time of the window function, e is a natural constant, t is time, and j is the imaginary number (Yan et al., 2021). A Hanning window length of 2056 and a time length of 20.56 s correspondingly is used. A built-in function “spectrogram” of MATLAB is used to achieve STFT directly from the software manual. The sampling rate is 100 Hz, so we choose 1 Hz and 50 Hz (i.e., a half of 100 Hz) as f_{\min} and f_{\max} .

C25: 260-261: specify that you perform the x-corr analysis between the seismic signals recorded at the stations in each site. Do you perform it on raw data or on the amplitude envelope? As I understood it is the second one but make it clearer.

R25: Thank you very much for your valuable comments. We used the amplitude method to process the entire debris flow signal. This approach helps to eliminate high-frequency noise and provides a more stable representation of the amplitude of the seismic signal. Using the entire debris flow signal, we calculated the average flow velocity based on the time delay and distance between the peak amplitude differences of the signals from two measurement points. This method effectively captures the flow characteristics by focusing on the peak amplitude differences between the measurement stations. As follows:

Lines 614 to 618

The sampling rate for seismic signal monitoring is 100 Hz. The average amplitude

for each second of seismic data is calculated using the amplitude method (Arattano, 1999), whereby 100 seismic signals are recorded within each second and their amplitudes are averaged. This method helps to smooth out high-frequency noise and provides a more stable representation of the amplitude of the seismic signal.

C26: 262-273: rewrite this removing the equation and explaining how and why you used the crosscorrelation analysis

278-281: I suggest removing the equation for PSD: it is well known spectral analysis

282-285: this is true but rephrase the sentence

R26: Thank you very much for your valuable comments. Based on the reviewer's suggestions, we have rewritten and simplified the Methods section, with a particular focus on explaining why this method was chosen. We have also added relevant references to support the changes. As follows:

Lines 241 to 270

3.1 Power spectral density analysis

Tsai et al. (2012) developed a PSD model for sediment transport that links seismic signals with water turbulence, precipitation, and sediment transport in rivers. In their model, they considered the relationship between seismic signals and the transport of bedload in rivers. Tsai et al. (2012) adapted this model for debris flows by including absorption damping during the propagation process and established the PSD model for debris flows near the source shown in Eq. (1). This model links debris flow parameters such as length, particle size, width, velocity, and attenuation factors (due to absorption) as well as viscoelastic parameters during propagation with the seismic PSD of the debris flow.

$$PSD \approx 1.9 \cdot LWD^3 u^3 \cdot \frac{f^{3+5\xi}}{v_c^5 r_0} e^{-\frac{8.8 f^{1+\xi} \eta}{v_c Q}}, \quad (1)$$

where W is width of the channel, D represents the 94th centile of the grain size distribution, u represents debris flow velocity, f is frequency, v_c is Rayleigh wave phase velocity at 1 Hz, r_0 is distance between the monitoring station and channel, L is effective length of $L=r_0$, $\xi=0.4$ is a parameter related to how strongly seismic velocities increase with depth at the site, and Q is an attenuation factor (Tsai et al., 2012; Lai et al., 2018).

Debris flow seismic Power spectral density calculated by Eq. (2), which means the power per frequency for different frequencies in a specific period (Yan et al., 2020), and allows debris flow evolution to be analyzed from the seismic signal. The power of full band seismic is calculated by the short-time Fourier transform (STFT, Eq. 3), allowing getting the frequency domain characteristics of the signal versus time, which can help us to get the PSD changes versus the time.

$$PSD_{f_{\min} \sim f_{\max}}(t) = \frac{1}{(f_{\max} - f_{\min})} \times \sum_{f=f_{\min}}^{f_{\max}} X(t, f), \quad (2)$$

$$X(t, f) = \sum_{m=-\infty}^{\infty} x(m)W(t - m)e^{-j2\pi fm} \quad (3)$$

where f is the angular frequency, f_{\min} and f_{\max} represent minimum frequency and maximum frequency, respectively, t is time for the seismic signal, $X(t, f)$ represents the spectrogram based on STFT (Yan et al., 2017)., x are time domain signals, W is the window function, m is the start time of the window function, e is a natural constant, t is time, and j is the imaginary number (Yan et al., 2021). A Hanning window length of 2056 and a time length of 20.56 s correspondingly is used. A built-in function “spectrogram” of MATLAB is used to achieve STFT directly from the software manual. The sampling rate is 100 Hz, so we choose 1 Hz and 50 Hz (i.e., a half of 100 Hz) as f_{\min} and f_{\max} .

Lines 307 to 316

3.3 Cross-correlation function And Manning formula

Arattano and Marchi (2005) found that the velocity values calculated using cross-correlation were close to the measured velocity values. In the context of debris flows, the average flow velocity between observation stations can be obtained by dividing the distance between the stations by the signal time delay. This method has been used to objectively calculate the mean velocity of debris flows (Coviello et al., 2015):

$$[x_K] = [x_0, x_1, x_2, \dots, x_{M-1}] \quad (6)$$

$$[y_K] = [y_0, y_1, y_2, \dots, y_{M-1}] \quad (7)$$

$$\phi_{yx}(\tau) = \sum_{t=0}^{M-1} x_t y_{t+\tau}, \quad (8)$$

where y from station 2 is another signal of time domain for the same event as x from station 1, t and K which are absolute sampling time series from 0 to $M-1$, ϕ represent cross-correlation function. When t exceeds $M-\tau-1$ and is less than 0, x_t and $y_{t+\tau}$ is equal to 0.

C27: Eq. 6: where does this eq come from? Please introduce it and explain why you present it in the text. The purpose is to compute some debris flow features from PSD? If so, write this. Anyway, previous theoretical and experimental studies indicate that the recorded seismic frequency depends on the source-to-receiver distance, which controls the recorded peak frequency (Tsai 2012, Kena 2015, Lai 2018, Belli 2022). The debris flow is a white source emitting almost all frequencies in the range of 1100 Hz. What you record depends on the propagation effects. Therefore it seems unrealistic to me using PSD to get info on flow parameters as the recorded frequency depends only on signal attenuation and results the same for different DFs recorded at the same site (Belli et al. 2022).

R27: Thank you very much for your valuable comments. Based on the reviewer's suggestions, we have rewritten and simplified the Methods section, with a particular focus on explaining why this method was chosen. We have made modifications, which can be found in **R26**.

C28: Section 3.4:

292: seismic energy and velocity?

295: energy loss is h? write this

300: what is Γ ? Please introduce the equation.

303-304: I don't understand this sentence

R28: Thank you very much for your valuable comments. We have rewritten this section. As follows:

Lines 271 to 306

3.2 Absorption attenuation compensation

During the actual propagation of seismic waves through geological layers, scattering and absorption attenuation effects occur, which means that the phase velocity and group velocity are different and the amplitude of the seismic waves is subject to

varying degrees of attenuation. This phenomenon has been well documented and studied in many related works (Futterman, 1962; Strick, 1967). In this study, we use the constant Q model (Kjartansson, 1979) to describe the absorption attenuation in the actual geological layers, and we have established a 1D plane wave amplitude attenuation equation for linear viscoelastic media (Eq. 4) to approximate the energy loss of seismic signals from debris flows during propagation. From this equation, it can be deduced that the amplitude of seismic waves is exponentially negatively correlated with both the propagation time and the frequency. In other words, as the propagation distance increases and the frequency rises, the amplitude of the seismic waves decreases significantly. This also explains why seismic signals from debris flows generally have lower frequencies when measured from greater distances.

$$h(t, f) = e^{-\frac{\pi f t}{Q} \left| \frac{\omega_0}{\omega} \right|^{\frac{2}{\pi} \arctan\left(\frac{1}{2Q}\right)}}, \quad (4)$$

where f is the frequency of the seismic signal, t is the spreading time (i.e., 0.02 s and 0.05 s) which is equal to distance r_0 between the monitoring station and channel divided by Rayleigh wave velocity v_c in Eq. (1), Q represents attenuation factor quantitatively depicting the absorption attenuation, and ω_0 and ω are reference angular velocity at 1 Hz ($\omega_0=2\pi$) and angular velocities, respectively.

Direct use of Eq. (4) to compensate for absorption attenuation results in significant attenuation in the high-frequency range, leading to a lower signal-to-noise ratio (SNR) and an excessively large amplitude compensation factor. This can cause the compensated amplitude to become too large and the SNR to be extremely low (Wang, 2002). In this study, I will use the gain control method proposed by Wang (2002) (Eq. 5) to maintain the stability of the high-frequency range. This method aims to improve the energy of the high-frequency range while keeping the overall SNR of the entire frequency band relatively controlled.

$$\Gamma(t, f) = \frac{h(t, f) + \sigma^2}{h^2(t, f) + \sigma^2}, \quad (5)$$

where σ is a constant named stability control factor, whose value comes from a numerical experiment., with a σ^2 value of 0.02 used here.

After applying absorption damping compensation according to Eq. (5), not all absorption damping terms in Eq. (1) are completely compensated. However, the partial compensation of absorption damping allows the PSD and the time-frequency characteristics of the seismic signal to reflect the changes in the characteristic parameters of the debris flow more accurately. This allows the PSD of the seismic signal of the debris flow obtained using Eq. (2) to be analyzed more effectively using Eq. (1).

C29: Section 4:

312: processing raw data? How?

End of 314-315: move this line at 312

317: figure 5?

321: instrument layout?

R29: Thank you very much for your valuable comments. We have rewritten this section. As follows:

Lines 330 to 348

Based on the instrument response data in Table 1, the original seismic data was corrected for the instrument response and converted to velocity (m/s). Through a joint analysis of the seismic signals recorded by the observation system on August 19, 2022, and precipitation data, we were able to determine that two debris flows occurred in Fotangba and one in Er Gully. All three debris flows were likely triggered by precipitation. As shown in Fig. 4, significant amplitude increases and fluctuations in the seismic signals were observed during the debris flows. By analyzing the wavefield characteristics of the debris flows, we were able to determine the approximate times of all three events. The rainfall record for Fotangba Gully shows hourly rainfall of 6.4 mm and 14.2 mm before the first and second debris flows, respectively (Fig. 4e). In Er Gully, the hourly rainfall before the debris flow was 3.8 mm (Fig. 4f). Analysis indicates precipitation occurred before the three debris flows. Additionally, the rainfall data can be linked to the initiation time of the flows and significant changes in seismic signals. The two debris flows in Fotangba Gully coincided with the maximum hourly rainfall on the day of the events (second highest and highest) within a 24-hour period, while the

Er Gully debris flow did not coincide with a maximum. However, the cumulative rainfall before the Er Gully debris flow reached 15 mm, greater than the cumulative rainfall for the first debris flow in Fotangba Gully. Therefore, rainfall is considered the triggering factor for debris flow initiation in both gullies.

C30: 322: how do you calculate SNR?

R30: Thank you very much for your valuable comments. We selected the seismic signals from the same time period on the day prior to the debris flow event as the background noise, and calculated the ratio of the debris flow signal power to the noise power as the signal-to-noise ratio (SNR). As follow:

Lines 354 to 357

We selected the seismic signals from the same time period on the day prior to the debris flow event as the background noise, and calculated the ratio of the debris flow signal power to the noise power as the signal-to-noise ratio (SNR) (Fu et al., 2020).

C31: 330: specify that you limit the analysis at the second event just for the Fotangba Gully; you also analyze the Er Gully event, right?

340-341: rainfall is a common trigger for debris flow. Your conclusion is reasonable but discuss it in the framework of the state of the art: our findings agrees with ...

R31: Thank you very much for your valuable comments. We have conducted a simple analysis of the debris flow occurrence time in Er gully using only seismic motion signals and rainfall data. However, the primary focus of the analysis remains on the second debris flow event in Fotangba gully. Rainfall data was primarily used to analyze the triggering factors of the debris flow. This study did not conduct an in-depth analysis of rainfall; the emphasis is still on the seismic signal analysis. Additionally, we have removed the rainfall analysis results from the Conclusions and Discussion sections.

C32: Figure 4: put circles with numeric labels on the 2 events in Fot. Gully toin (a) and (c) make easier to see the two events: it is not clear that a and c shows 2 events. You can also state this in the caption

R32: Thank you very much for your valuable comments. We have made modifications.

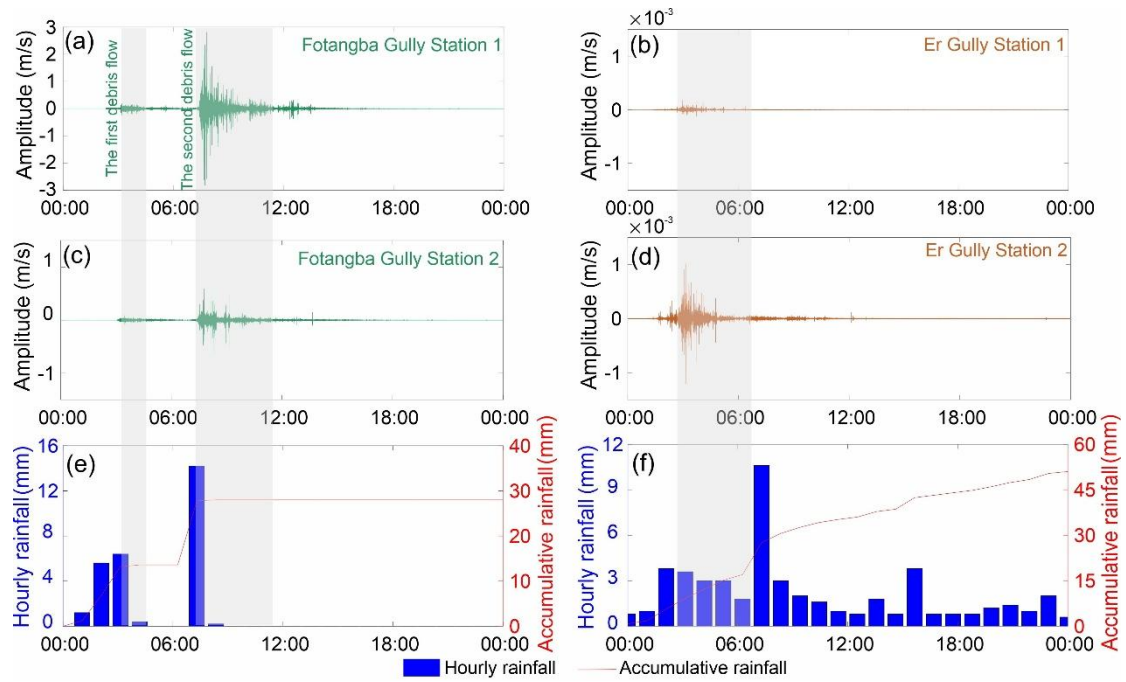


Fig. 4. Raw seismic signals and rainfall data. (a) and (c) represent monitoring station 1 and station 2 in the Fotangba Gully; (b) and (d) represent monitoring station 1 and station 2 in the Er Gully; (e) Rainfall at Fotangba Gully; (f) Rainfall at Er Gully.

C33: 4.1.2: I am not an expert, but this procedure to recover the original signal does not appear reliable to me and seems too simplistic approach. In addition, it is not clear to me how the propagation effects are cancelled. Did you also account for geometrical spreading? Also, you use σ_2 computed at 1 Hz but the seismic signal are mostly above 10 Hz (Figure 5). Here equations should help: $\text{Signal restored} = \text{signal recorded} * h$

R33: Thank you very much for your valuable comments. We employed Eq. 7(Eq. 4) to compensate for the frequency-dependent energy attenuation. We did not compensate for other forms of energy loss, such as geometrical spreading mentioned by the reviewer. This is because geometrical spreading affects all frequencies equally, and since the positions of our sensors and the river channel remained unchanged, the geometrical spreading effect is uniform across the entire debris flow signal. The compensation for geometrical spreading would be equivalent to multiplying the amplitude by a fixed value, as suggested by the reviewer in the form of $\text{Signal restored} = \text{signal recorded} * h$. Given that all our analyses are based on a linear system, multiplying by a constant factor results in an overall change in amplitude but does not affect the relative changes. Our primary focus in the subsequent analysis is on the power spectral density (PSD) energy at different frequencies. Therefore, it is necessary to compensate for the absorption attenuation effects that vary with frequency. However, we acknowledge that our compensation cannot completely eliminate propagation effects. For instance, the high-

frequency stability factor may lead to insufficient compensation for high frequencies, and the actual formation absorption attenuation factor Q cannot be accurately obtained. These inherent limitations prevent us from fully eliminating propagation effects. Nevertheless, our approach can partially mitigate the impact of propagation effects on the seismic signal, allowing the PSD energy obtained from Eq. 5 (Eq. 2) to be closer to

that in Eq. 6 (Eq. 1) (excluding $\frac{f^{3+5\xi}}{v_c^5 r_0^5} e^{-\frac{8.8 f^{1+\xi} \eta}{v_c Q}}$). This enables us to analyze the characteristics of the debris flow based on $PSD \approx 1.9 \cdot LWD^3 u^3$. The 1 Hz we refer to is the choice of 1 Hz as the reference frequency, corresponding to the frequency of v_c in Eq. 6 (Eq. 1).

C34: 358-359: as I understand you use a total of 50 m, so it should be 25 m upstream and 25 m downstream. Anyway, limiting your procedure only to this short channel section seems incorrect to me. As you too wrote, a debris flow is an extended moving source and what you recorded is the result of the contribution of the signal components produced in different sections of the channel and in different times. The signal produced in the short section in front of the seismometer almost only corresponds to a short duration window of the all signal. You use the parameters of this section to reconstruct the all signal which is mostly produced in several other channel portions.

R34: Thank you very much for your valuable comments. The reviewer raised a very pointed question. Of course, if we could model the entire river channel morphology and the velocities around the channel, it would be extremely helpful for obtaining the most effective compensation results. However, this process is prohibitively expensive and difficult for us to accomplish. Discussing the path calculation and range selection separately would be a complex topic that warrants a dedicated paper, and it is not the core objective of this paper.

We chose a range of 25 meters upstream and 25 meters downstream as the primary source area for the sensors to receive signals. This selection aims to capture the most influential segment to approximate the propagation path of the debris flow, thereby achieving a certain degree of compensation for the different attenuation levels of various frequencies in the debris flow signal caused by geometrical spreading.

C35: 380-386: I don't understand this paragraph

R35: Thank you very much for your valuable comments. In this study, we performed numerical calculations by continuously adjusting the compensation parameters. When the compensated data stabilized, meaning there was no significant difference between

the trend of the compensated signal and the original signal, and the overall consistency was maintained, we considered the numerical experiment to be stable at that point.

C36: 389: why are attenuation at station 1 and 2 so different? Why is it larger at 2?

R36: Thank you very much for your valuable comments. This is mainly related to the geological conditions and installation locations of the observation stations. Observation Station 2 is located closer to the center of the channel.

C37: Figure 5: adding labels with “Fotangba Gully” and “station 1” and “station 2” in the corresponding plots should help a fast understanding of the figure

410-411: trivial

433: rephrase as: “to investigate the seismic manifestation of the evolution of the second debris flow...”

441: not clear if the frequency passed from 8 to 43 Hz or if it is between 8 and 43 Hz. Clarify this.

R37: Thank you very much for your valuable comments. We have made modifications. As follow:

Lines 434 to 466

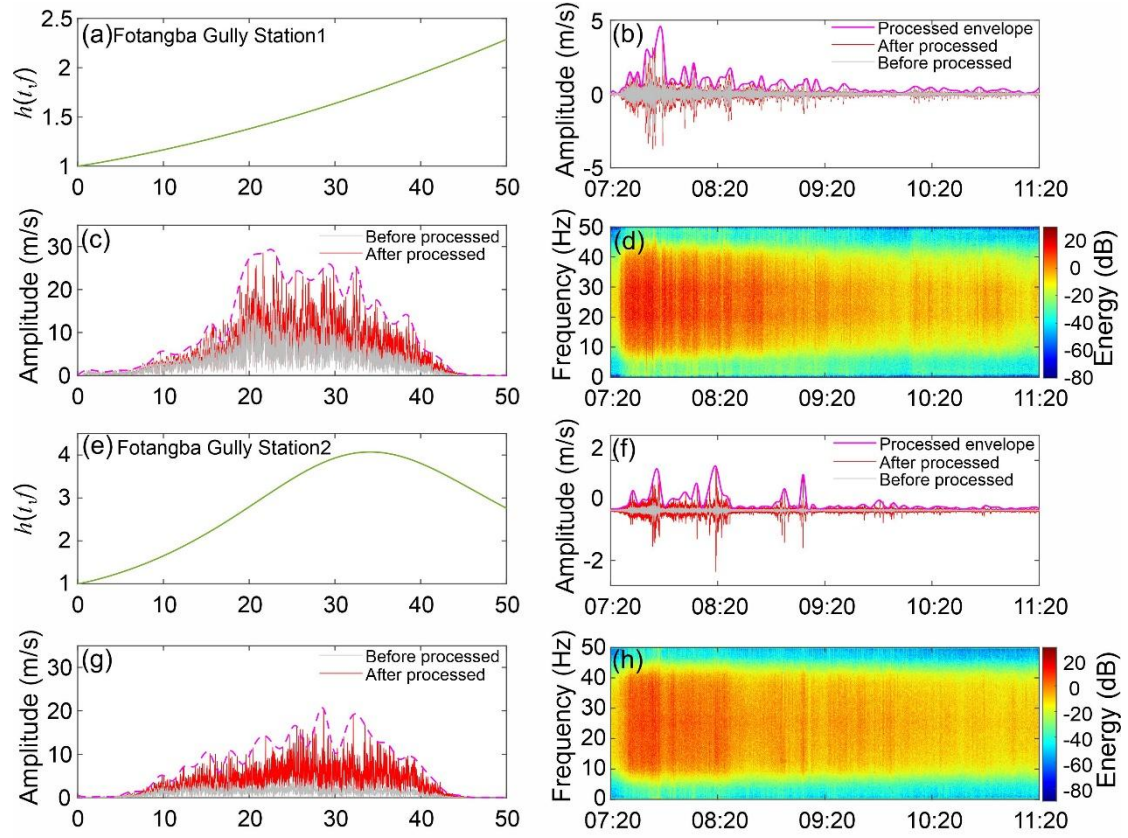


Fig. 5. Restored seismic signal for the second debris flow in Fotangba Gully. (a) Compensation function curve for monitoring station 1; (b) Time domain signal at monitoring station 1; (c) Frequency domain signal at monitoring station 1; (d) Restored spectrogram for monitoring station 1; (e) Compensation function curve for monitoring station 2; (f) Time domain signal at monitoring station 2; (g) Frequency domain signal at monitoring station 2; (h) Restored spectrogram for monitoring station 2. The red dashed lines in (c) and (g) are envelopes that represent peak amplitudes after processing.

At monitoring point 1, the signal amplitude and frequency range rapidly increased when the debris flow occurred. The frequency range primarily concentrated between 8 Hz and 43 Hz. During the debris flow event, the energy initially concentrated and then gradually decreased, with a range between -120 dB and -60 dB. The data from monitoring point 2 was essentially consistent with that from monitoring point 1, recording the debris flow starting at 7:26 AM, with a peak amplitude observed around 7:45 AM, followed by a gradual decline. However, there were minor differences in the frequency bandwidth at monitoring point 2, which concentrated between 10 Hz and 40 Hz. The energy variation trend and range were almost the same as those at monitoring

point 1. Throughout the entire debris flow event, the observed peak frequencies at the two monitoring points were 21.6 Hz and 28.6 Hz, respectively. The frequency evolution between the two points indicates an increase in the peak frequency, which may be related to changes in particle impacts and scale. Factors such as rock falls and channel erosion might also influence the peak frequency. To reflect the surge wave characteristics, we used the upper envelope of the signal waveform (Fig. 5b and 5f). The surge waves corresponded with the wave characteristics of the debris flow, and the number of surges matched the number of waves. The flow depth between the surge waves was significantly discontinuous, with a sudden increase in flow depth from one surge to the next, similar to the characteristics of the surge flow. Monitoring point 1 observed about 8 significant surge waves, while monitoring point 2 recorded 7. Additionally, we noticed that monitoring point 2 recorded two significant surge waves around 9:00 AM, while monitoring point 1 did not observe any significant surges at the same time. This indicates that the flow dynamics of the debris flow between the two monitoring points along the river channel have changed, possibly due to variations in channel topography and the solid-phase content of the debris flow.

C38: 447: the seismic peak amplitude phase reflect the passage of the debris flow front in the closest point to the sensor (Marchetti 2019, Walter 2017, Belli 2025, Coviello 2019), and not an increased magnitude of the event. The source is moving along the channel. The boulder rich front dominates the seismic signal.

R38: Thank you very much for your valuable comments. Indeed, “The boulder-rich front dominates the seismic signal,” which is indeed very accurate for near-source observations, especially when the average flow velocity of the debris flow changes. During propagation, the energy at each frequency decreases to varying degrees, with higher frequencies being attenuated more significantly. Therefore, the reviewer's comment, “The seismic peak amplitude reflects the passage of the debris flow front at the closest point to the sensor, not an increased magnitude of the event,” is extremely accurate. However, for near-source observations, since the propagation distance is relatively short, the high-frequency attenuation is weaker, and we are able to capture changes in high-frequency information. Thus, analyzing debris flow changes using near-source data is also feasible. If the debris flow is large enough, we can observe low-frequency signals similar to landslides from long distances (over 100 km). In summary, debris flow signals are not white noise; both near-source and far-source observations

have their unique characteristics, though long-distance observation is generally more challenging. Additionally, as mentioned by Belli (2025), “For a complete characterization of the debris-flow seismicity, a comparative analysis with the boulder size would be required too, because grain size has been shown to be a dominant controlling factor in impact-generated seismic waves (Tsai et al., 2012).” In our analysis, the changes observed for the same station mainly reflect variations in debris flow velocity, particle size, and flow rate, while other factors like propagation distance, geological conditions, and river width are kept constant. This is also one of the reasons why we attempt to qualitatively analyze the changes in debris flow characteristic parameters by examining the variation in PSD features at different times.

C39: 449-451: “potentially due to varying particle impacts and scale”: more likely the varying peak frequencies reflects variations in the source-to-receiver distance: the closest station should show the higher peak amplitude (Tsia 2012, Kena 2015, Belli 2022). Belli 2022 clearly showed that the seismic peak frequency of several events is the same regardless of flow parameters.

R39: Thank you very much for your valuable comments. Indeed, the propagation distance controls the peak frequencies, and this is based on the scenario where multiple sensors at different stations observe the same debris flow. The closest station should exhibit the higher peak amplitude and peak frequency. For the same station, as the debris flow velocity increases, the flow rate becomes larger, and the particle concentration and particle size increase, the peak frequency will also increase. This is consistent with Eq. 6 (Eq. 1), which shows that PSD has a negative exponential relationship with propagation distance and a cubic relationship with particle size and velocity. PSD is influenced by the combined effect of these factors. Therefore, studying particle impacts and scale through the PSD variation at different times, while keeping the propagation distance fixed, is also reasonable.

C40: 467-468: but you should have removed the propagation effects, no?

Figure 7: if I am correct, these plots are already shown in Figure 5, why do you repeat them?

R40: Thank you very much for your valuable comments. We used the compensation function to restore the high-frequency signals of the debris flow as much as possible. However, it is impossible to completely eliminate the path propagation effect, so only partial restoration was achieved. Fig. 7 was redundant, so we have removed it.

C41: Section 4.2: More details are needed: do you compute the x-corr on the entire signal duration or on subsequent signal windows (specify this in the Method, see comments above)? It would be nice to see a plot of the x-corr on a time-lag (XY)

diagram (like those in Ichihara 2012 or Belli 2025): this could enable to see variation in the flow velocity if a varying lag is observed through time.

R41: Thank you very much for your valuable comments. We used the amplitude method to process the entire debris flow signal. This approach helps to eliminate high-frequency noise and provides a more stable representation of the amplitude of the seismic signal. Using the entire debris flow signal, we calculated the average flow velocity based on the time delay and distance between the peak amplitude differences of the signals from two measurement points. This method effectively captures the flow characteristics by focusing on the peak amplitude differences between the measurement stations. As follows:

Lines 614 to 618

The sampling rate for seismic signal monitoring is 100 Hz. The average amplitude for each second of seismic data is calculated using the amplitude method (Arattano, 1999), whereby 100 seismic signals are recorded within each second and their amplitudes are averaged. This method helps to smooth out high-frequency noise and provides a more stable representation of the amplitude of the seismic signal.

C42: 477: suggestion: Debris flow velocity “estimation” instead of “analysis”

480-483: remove this, repetition (478-480)

484: Comiti et al., 2014 perform cross-correlation on flow depth measurements

500-502: rephrase this

500: what is this? RMSA (root mean square amplitude)? Amplitude envelope? Explain this and add it to the method section if necessary

R42: Thank you very much for your valuable comments. We have made modifications, which can be found in **R41**.

C43: 508: what values of tau and r you used to get 38.3 km/s?

R43: Thank you very much for your valuable comments. We used the same method to calculate the velocity of the Er gully debris flow. For specific information about the Er gully observation station, please refer to [Section 2.1](#).

C44: Figure 8: show a plot of cross-correlation through time (like those in Ichihara 2012 or Belli 2025): this could enable to see variation in the flow velocity if a varying lag is observed through time.

R44: Thank you very much for your valuable comments. [Fig. 8a](#) shows the signal delay.

C45: 519-520: show the Manning formula. I don't know if this is applicable for debris flows, where the extreme particle transport affects flow dynamics, or just to water flows.

R45: Thank you very much for your valuable comments. The Manning formula can be used to calculate the velocity of debris flows. As follows:

Lines 317 to 319

The Manning formula ([Eq. 9](#)) is used to calculate the peak flow velocity of a debris flow passing through a section, based on characteristic terrain parameters of the section ([Yu and Lim, 2003](#); [Cui et al., 2013](#); [Guo et al., 2016](#)).

C46: Table 3: why are the manning formula values missing for event 1 and 3

Section 4.3: rephrase the title

537-540: rephrase the period

Section 4.3.1: this section is too long and results boring and difficult to follow. Shorten it keeping only the key aspects.

573-578: you state that images match seismic data: but with seismic data you just reconstruct several surge and gave a velocity estimate so far. No other info was retrieved.

599: bottom? Isn't it apex?

R46: Thank you very much for your valuable comments. Due to the missing image data from the other two debris flow events and the damage that occurred at the site afterwards, we were unable to accurately obtain all the parameters for the Manning formula. As a result, we did not use the Manning formula for calculations. Additionally, since the time interval between images captured by the delay cameras is 5 minutes, there are numerous image data points. Therefore, we did not conduct a detailed analysis of all the images. Instead, we selected specific time periods corresponding to wave surges for analysis, in conjunction with the seismic signals. Other relevant content has also been revised.

C47: 603: how can a 4.3 kg sample be representative of a debris flow deposit where several boulders up to a few meters in diameter are present? What about bigger rocks, which also dominate the seismic signal? I think this granulometric analysis is biased by the sampling method. You sampled the matrix not the deposit. What is important for the seismic signal are mostly the larger boulders ([Kean 2015](#), [Walter 2017](#), [Coviello 2019](#), [Marchetti 2019](#) ecc).

R47: Thank you very much for your valuable comments. Indeed, the seismic amplitude generated by individual large boulders is significantly larger than that from smaller particles. The particle size distribution (PSD) is influenced by factors such as flow velocity, and the largest portion, which consists of the smaller particles, plays a dominant role in determining the overall signal characteristics. This approach is similar to that used by [Lai \(2018\)](#), who relied on D_{95} (the particle size below which 95% of the particles fall) in deriving the PSD for debris flows, though this specific value might need verification. When observing the accumulation body, we found that large boulders are relatively rare. For our analysis, we performed vertical sampling at a specific location, covering different stages of the debris flow. This approach allowed us to capture a representative range of particle sizes, which in turn provided a more accurate reflection of the overall characteristics of the debris flow's particles.

C48: Section 4.3.3: PSD in Figure 12 a are really smoothed for being computed on raw seismic data. How do you computed them? Signal window of analysis? Smoothing applied? Specify this in the methods. The D values are too low for a debris flow a not representative of the seismic source. It is not corrected using particles with a maximum of 2.5 cm diameter for computing the PSD of the seismic signal produced by a debris flow. I suggest repeating the analysis with more senseful D values. Also the recorded seismic frequency only depends on propagation effects: using it to get information on the particle size or velocity is highly speculative and incorrect. As I said before, I don't think that the signal correction you performed eliminated the propagation effects from the signals. The results are highly speculative and not supported by independent evidences.

R48: Thank you very much for your valuable comments. In [Fig. 12a](#) ([Fig. 10a](#)), we performed calculations based on [Eq. 5](#) ([Eq. 2](#)), the calculation time window is 30 seconds before and after that moment. The choice of a maximum of 2.5 cm is based on post-event survey data, where the D_{94} particle size was found to be 0.018 m. Using this particle size, we calculated the debris flow velocity to be 7.9 m/s using the Manning formula, which is quite consistent with the velocity of 7.0 m/s calculated using cross-correlation. This further supports the reasonableness of analyzing using a D_{94} particle size around 0.18 m. The 2.0 cm and 2.5 cm values we used refer to the D_{94} particle size. Indeed, our compensation cannot completely eliminate the path effect. Since the high-frequency part of the signal already has a low signal-to-noise ratio (SNR), the SNR further decreases during propagation. The absorption compensation can only adjust the energy across different frequency bands but cannot improve the SNR. The goal of compensation is to reduce the impact of path effects on the seismic signal. Propagation effects alter the characteristics of seismic signals, such as the relative energy in each frequency band and the peak frequency. However, the seismic signal characteristics of the debris flow are still determined by the flow characteristics themselves. Propagation effects only change the signal's features. By eliminating propagation effects and

considering conditions where the effects from a single station are nearly the same, we can analyze the changes in PSD characteristics at different times to assess particle size or velocity.

C49: 627: What are time points?

628: whose infrared images?

R49: Thank you very much for your valuable comments. We have made modifications. As follow:

Lines 664 to 665

PSD curves for six time points, corresponding to their infrared images (Fig. 7b to 7h), were calculated using Eq. (2) (Fig. 10a).

C50: 633-636: it seems to me that the PSDs show almost the same trend at the different times: only the amplitude changes. High and low frequencies show the same trend (the one you described for the low frequencies).

R50: Thank you very much for your valuable comments. Indeed, the overall trend of the PSD curve for a single time period is consistent, but the changes at the peak and minimum points differ across different time periods. Therefore, in our analysis, we are comparing the variations in the high-frequency and low-frequency ends of different curve segments. The focus is on comparing the curves from five different time periods, rather than analyzing a single curve.

C51: 642: these grain sizes are unrealistic for a debris flow and result from a wrong sampling method (see above). In addition, the seismic signal is dominated by the larger boulders. Computing the PSD using diameters up to 2.5 cm is not representative of the most energetic seismic source in DFs. Indeed you get PSD at -110 dB compared to the recorded one which is at -70 dB.

R51: Thank you very much for your valuable comments. Our choice of particle size and velocity is based on field survey data and the debris flow velocity calculated through cross-correlation. For a detailed response, please refer to **R48**.

C52: 654: which one? The real of the synthetic one? Specify

R52: Thank you very much for your valuable comments. This refers to the actual PSD curve, which we have modified.

Lines 664 to 665

PSD curves for six time points, corresponding to their infrared images (Fig. 7b to 7h), were calculated using Eq. (1) (Fig. 10a).

C53: 654-655: highly speculative

R53: Thank you very much for your valuable comments. Examining the PSD curves for the six time points reveals a gradual decrease in energy at the high-frequency end ($>25\text{Hz}$). For example, the PSD energy at 30 Hz is highest at 7:39, and is lower at all other time points. This indicates a reduction in the quantity of particles generating high-frequency energy, suggesting that both the number of larger particles and their movement speed are decreasing. The reduction in particle quantity and velocity is mainly due to the decrease in flow velocity, which in turn reduces the debris flow's carrying capacity. This is the reasoning behind the conclusion stated in the original text. We kindly ask the reviewer to examine and verify this explanation."

C54: 659: the same is observed for high frequencies!

R54: Thank you very much for your valuable comments. In this revised version, we have modified it as below.

Lines 674 to 677

The PSD of high frequency decreased rapidly from 7:39 to 7:47, while a spike in low frequency occurred from 7:39 to 7:44, followed by a quick drop from 7:44 to 7:54. The frequency changes during the rest of the time were not significant.

C55: 662: the recorded peak frequency results from the source-to-receiver distance

R55: Thank you very much for your valuable comments. Peak frequency is determined by both the debris flow characteristics and the source-to-receiver distance. When the source-to-receiver distance is the same, the peak frequency is primarily controlled by both particle size and flow velocity (Eq. 1).

C56: 669: the variation is very small (2-3 Hz) and I don't know if it is representative of the source or depends on data analysis.

R56: Thank you very much for your valuable comments. Indeed, this change is minimal. During the evolution of the debris flow, the variation in characteristic parameters over short periods is typically small, which aligns with the nature of the debris flow. Since there was no change in the station, we do not consider the source-to-receiver distance factor.

C57: 670: this is not true: generally, as velocity increases, it increases the diameter of the transport particles, if still available, because the flow has more transport capability.

R57: Thank you very much for your valuable comments. There was an error in the expression of this section, and we have made revisions.

Lines 717 to 730

The seismic signals received from the debris flow with a high velocity, massive volume, and rich particle content primarily consist of low frequencies with lower peak frequencies. Conversely, the signals are mainly high frequencies under the opposite conditions. The low- and high-frequency energy shows a substantial enhancement from 7:44 to 7:49, along with an alteration in the peak frequency toward a higher frequency, indicating an increasing signal strength at different propagation distances. In contrast, low-frequency energy decreases and high-frequency energy stays stable at 7:54, suggesting that the seismic energy from distant sources weakens and from nearby sources remains steady. The variation of grain concentration (flow volume and particle content) near the channel affects the shape of PSD. An anomaly observed at 7:44 in low-frequency energy is due to the upstream flow volume rising. As debris flow with high grain concentration moves toward the sensors and flows downstream, the low-frequency energy decreases and eventually recovers to a normal level.

C57: Figure 12: (a): not clear how these curves are computed (signal window, smoothing...). (b) not clearly readable: I suggest to make 2 different plots: one for the different D, the other for different velocities.

R57: Thank you very much for your valuable comments. For detailed calculations of the Figure 12a (Fig. 10a) curve, please refer to **R26**. We have replaced Figure 12b (Fig. 10b) with the new one to explain the mechanism of the curve shape change in Figure 12a (Fig. 10a).

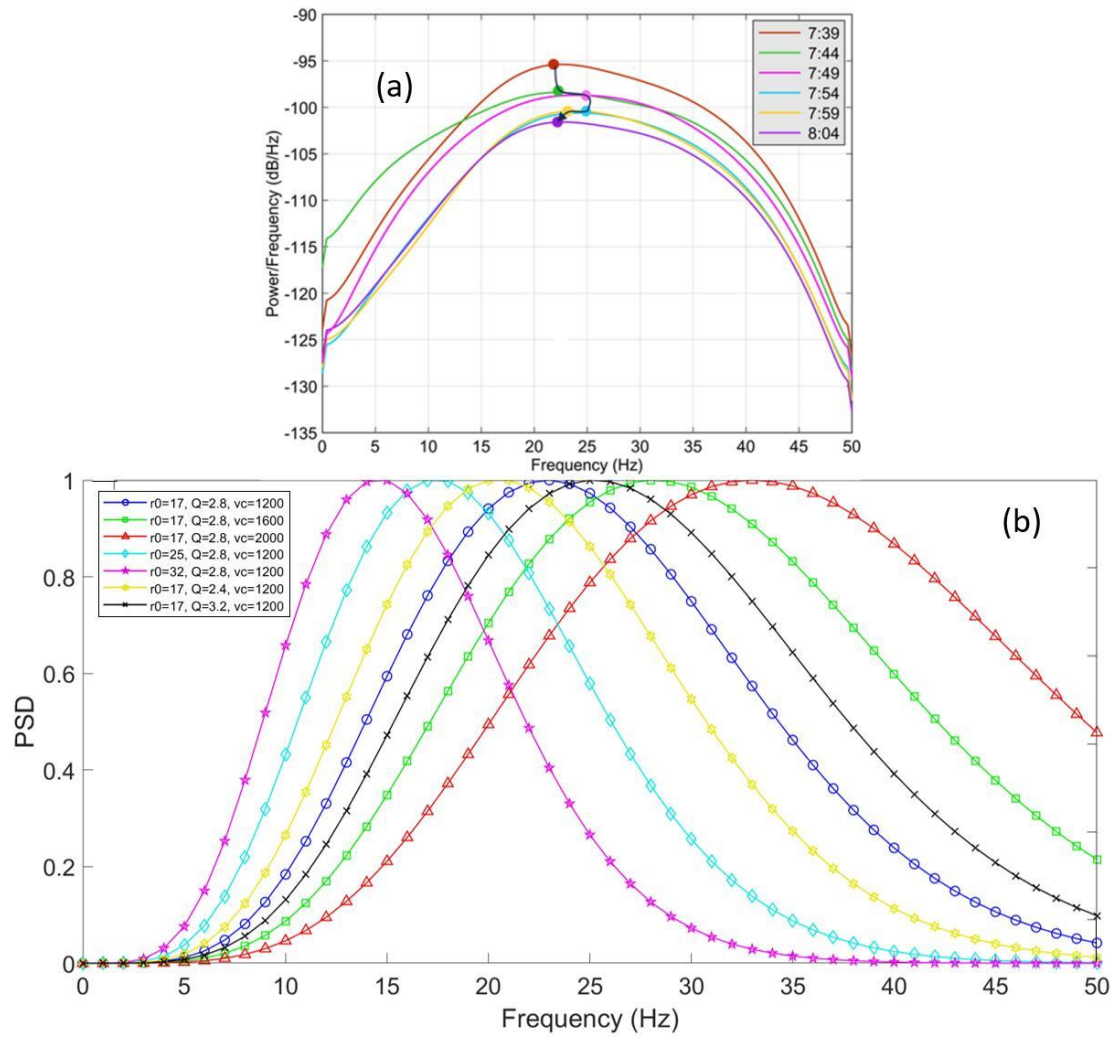


Fig. 10. Characteristic change of power spectral density (PSD). (a) Evolution of PSD during the second debris flow in Fotangba Gully on the morning of August 19, 2022, from 7:39 to 8:04; (b) Comparison of PSD for different r_0 , Q , and vc . The six dots in subplot (a) correspond to the PSD maximum at the six-time points from 7:39 to 8:04, and the black arrows indicate the time course of these six-time points.

C58: 682-684: you can't say this, you have no evidence.

683-684: contradiction: flow velocity decreases and later first increases and the decreases.

R58: Thank you very much for your valuable comments. We have made modifications. As follow:

Lines 678 to 692

The amplitude of PSD shows a gradually decreasing trend, reflecting that the flow velocity of debris flows as a whole shows a decreasing trend. D94 grain size, flow velocity, width and length of the channel only influence the PSD amplitude (Eq. 1),

while r_0 , v_c , and Q affect the shape of the PSD. The parameter, width and length of debris flow which are positively correlated with flow velocity given the short duration of the event, mainly characterize the flow volume, which is determine the volume of particle hitting the riverbed, and has a linear relationship with the PSD amplitude. We assumed that D_{94} grain size is proportional to flow velocity, given that starting velocity is proportional to the square of the particle size and the force maintaining the movement of particles is much smaller. So, the amplitude is reckoned to be scaled to the sixth power of the flow velocity (Eq. 1). Based on the above analysis, we can consider that the PSD energy is mainly controlled by the flow velocity of the debris flow. The amplitude of PSD showing a gradually decreasing trend, reflect that the flow velocity of the debris flow is gradually decreasing, and the extent of the debris flow speed reduction is gradually decreasing.

C59: 721-724: this is true, however you use preliminary results to extrapolate detailed information on the debris flow, with no strong independent evidences supporting your conclusions.

748-750: I don't understand this sentence

763-765: numerical stability: I think a better explanation should be given.

768: your work does not demonstrate anything for the real time monitoring.

R59: Thank you very much for your valuable comments. We have adjusted the focus of the study from monitoring and early warning to process reconstruction and feature analysis. The relevant content has already been modified.

C60: Some technical corrections (all text requires language revision):

Line 26: loss TO life...

Line 29: remove "to electricity and batteries"

Line 31-32: repetition: monitoring ... monitoring

Line 39: change "reconstruct" with "characterize"

Line 60-61: remove "early warining", "and evolve", "based"

Line 70-71: rephrase

Line 79-80: rephrase

Line 97-98: rephrase

Line 99: change “movement” with “debris-flow”

Line 104: “while” instead of “and”

Line 105: “localization” instead of “location”

110: rephrase as “...propagation distances, and therefore are often recorded only by close-range

instruments (Zhang 2021).” Specify how close.

117-118: rephrase as: “Unlike landslides, debris-flow seismic signals lack significant low-freq.

features, making remote monitoring impractical”

119: rephrase as “and their source processes is still limited”

130: rephrase

131: “consists” instead of “is compised”

133-135 rephrase

639: “We computed theoretical seismic PSD...” something like this

717-719: rephrase

R60: Thank you very much for your valuable comments. Based on your suggestions, we have rechecked the entire manuscript and made revisions.